American Mineralogist, Volume 88, pages 387–397, 2003

Fe^{2+}-Mg partitioning between garnet, magnesiowüstite, and $(Mg,Fe)_2SiO_4$ phases of the transition zone

DANIEL J. FROST*

Bayerisches Geoinstitut, Universität Bayreuth, D-95447 Bayreuth, Germany

ABSTRACT

The partitioning of Fe and Mg between garnet coexisting with olivine, wadsleyite, ringwoodite and magnesiowüstite solid solutions has been measured between 9 and 19 GPa and 1400–1700 °C. In addition to studying exchange reactions involving the pyrope-almandine garnet solid solution, majoritic garnets forming in a natural peridotite bulk composition have been also examined. Metallic Fe was added to all bulk compositions to buffer the Fe^{3+} concentration at its lowest possible level. Partitioning data between pyrope-almandine garnet and ringwoodite were combined with data for garnet-magnesiowüstite and ringwoodite-magnesiowüstite partitioning to refine thermodynamic mixing properties for these solid solutions at 18 GPa and 1400 °C. A multiple non-linear regression employing cation exchange data between these 3 solid solutions yielded the following well-constrained values for the differences in symmetric solid-solution interaction parameters: $W^{mw}_{FeMg} - W^{ring}_{FeMg}$ = 8.8(2) kJ/mol, $W^{mw}_{FeMg} - W^{gt}_{FeMg}$ = 12.8(5) kJ/mol, $W^{ring}_{FeMg} - W^{gt}_{FeMg}$ = 4.0(4) kJ/mol.

These differences were then solved simultaneously to give, on a single site basis: W^{mw}_{FeMg}= 13.2(3) kJ/mol, W^{ring}_{FeMg} = 4.4(2) kJ/mol, W^{gt}_{FeMg} = 0.3(3) kJ/mol.

In a peridotite composition, the occurrence of majorite and grossular garnet components produced a measurable influence on the Fe-Mg partitioning, however, the combined effect was relatively small because each individual component affected the partitioning in an opposite direction. These data, combined with previously determined phase relations in the Mg_2SiO_4-Fe_2SiO_4 system, were used to calculate the influence of garnet Fe-Mg partitioning on the pressure intervals of divariant $(Mg,Fe)_2SiO_4$ phase transformations in the transition zone. Results show that the presence of garnet reduces the pressure interval over which the $(Mg_{0.9},Fe_{0.1})_2SiO_4$ olivine to wadsleyite transformation occurs in a peridotite composition to 0.35 GPa (10 km) in comparison to 0.5 GPa in a garnet-free system. This width, however, is still greater than the estimated width of 4 km for the 410 km discontinuity observed in some regions of the Earth as inferred from high frequency reflected and converted seismic waves. The existence of garnet in a peridotite composition in the mantle cannot, therefore, be the only explanation as to why the 410 km discontinuity is, in some regions of the Earth, apparently sharper than experimental estimates for the $(Mg_{0.9},Fe_{0.1})_2SiO_4$ olivine to wadsleyite transformation. The wadsleyite to ringwoodite transformation is reduced to 0.8 GPa (25 km) compared to 1 GPa in the garnet-free system.

INTRODUCTION

Garnet is likely to be the second most abundant mineral throughout the transition zone and much of the upper mantle (Ringwood 1991). Over this range of stability, the composition of garnet will change significantly due to the influence of pressure on the partitioning relations between garnet and the other minerals of the mantle (Akaogi and Akimoto 1977; Irifune 1987; Irifune and Ringwood 1993; Irifune 1994). There are, not surprisingly, several reasons why it is important that we can predict the likely composition of garnet over a range of conditions. Recent studies have shown, for example, that the pressure interval of the divariant $(Mg,Fe)_2SiO_4$ olivine to wadsleyite transformation will be significantly narrowed in the presence of garnet due to the difference in Fe-Mg partitioning between garnet and each $(Mg,Fe)_2SiO_4$ phase (Stixrude 1997; Irifune and Isshiki 1998). The 410 km seismic discontinuity, which is believed to be caused by the olivine to wadsleyite transformation, is observed seismically to be very sharp and, in some regions of the Earth, appears to occur over a pressure interval of less than 0.2 GPa (Benz and Vidale 1993). This sharpness is apparently at odds with experimental estimates of the pressure interval of this divariant reaction, which are closer to 0.5 GPa (Katsura and Ito 1989; Fei and Bertka 1999). The presence of garnet in the mantle, which is a significant sink for Fe and Mg, could therefore explain this difference between the experimentally and seismically determined transformation intervals. An accurate knowledge of the partitioning relationships between garnet and other minerals is also required for thermobarometric calculations for the depth of origin of proposed ultra high-pressure peridotite terranes, mantle xenoliths, and inclusions in diamond (Van Roermund et al. 2001; Harte et al. 1999).

Here I report measurements of Fe and Mg partitioning be-

* E-mail: Dan.Frost@uni-bayreuth.de

tween the pyrope-almandine garnet solid solution and ringwoodite, wadsleyite, olivine, and magnesiowüstite solid solutions between 9 and 19 GPa and 1400–1700 °C. These data have been used to refine activity-composition relations for the garnet, ringwoodite, and magnesiowüstite solid solutions at high pressure. A peridotitic system has also been examined to determine how Fe-Mg partitioning may be influenced by the presence of grossular and majorite components in garnet.

The main complications in such a study arise from the very slow rate of cation diffusion in garnet and from the necessity to control the oxygen fugacity and consequently levels of Fe^{3+}. Many previous high-pressure experiments have been performed for relatively short run durations and reversal experiments have generally not been made. The attainment of equilibrium has therefore been questionable. The use of noble metal capsules and $LaCrO_3$ furnaces by some experimenters probably also results in high levels of Fe^{3+} in run products, which are likely to be incompatible with Fe^{3+} contents of the mantle. In a previous study it was shown that wadsleyite synthesized in the multianvil using a Re capsule and $LaCrO_3$ furnace but in the absence of an oxygen buffer could have an $Fe^{3+}/\Sigma Fe$ ratio as high as 30% (Frost et al. 2001). The $Fe^{3+}/\Sigma Fe$ ratio of the mantle, on the other hand, is probably on the order of 2%, which in the transition zone would result in an oxygen fugacity close to the Fe-"FeO" redox buffer (O'Neill et al. 1993). In this study, presynthesized garnet and olivine starting compositions were used that approached equilibrium from both higher and lower initial Fe contents, thus demonstrating equilibrium. Mixtures of garnet and olivine in a 5:1 mass ratio were employed such that the garnet composition had to change much less in comparison to the $(Mg,Fe)_2SiO_4$ polymorph. Longer run durations than most previous studies were also used. The oxygen fugacity was kept at its lowest level by the addition of powdered metallic Fe to the starting materials so that Fe^{3+} concentrations were low.

THERMODYNAMIC BACKGROUND

The partitioning of Fe and Mg between garnet and an $(Mg,Fe)_2SiO_4$ polymorph, be it either olivine, wadsleyite, or ringwoodite, can be represented on a one site basis by the exchange reaction:

$$\underset{\text{garnet}}{MgAl_{2/3}SiO_4} + \underset{\text{ringwoodite}}{FeSi_{1/2}O_2} = \underset{\text{garnet}}{FeAl_{2/3}SiO_4} + \underset{\text{ringwoodite}}{MgSi_{1/2}O_2} \quad (1)$$

The equilibrium distribution coefficient K_D for this reaction is defined as:

$$K_D = \frac{X_{Mg}^{ringwoodite} X_{Fe}^{garnet}}{X_{Mg}^{garnet} X_{Fe}^{ringwoodite}} \quad (2)$$

where X_{Fe}^{garnet} is either the molar Fe/(Fe + Mg) ratio or the Fe/(Fe + Mg + Ca) ratio. At equilibrium, the standard state free-energy change for exchange Reaction 1 is:

$$\Delta G^0(1) = -RT \ln \frac{a_{MgSi_{1/2}O_2}^{ringwoodite} a_{FeAl_{2/3}SiO_4}^{garnet}}{a_{MgAl_{2/3}SiO_4}^{garnet} a_{FeSi_{1/2}O_2}^{ringwoodite}} \quad (3)$$

taking the standard state to be the pure phases at the pressure and temperature of interest. The activities of the components are defined as:

$$a_{FeAl_{2/3}SiO_4}^{garnet} = (X_{Fe}^{gt} \cdot \gamma_{Fe}^{gt}) \quad (4a)$$

$$a_{FeSi_{0.5}O_2}^{ringwoodite} = (X_{Fe}^{ring} \cdot \gamma_{Fe}^{ring}) \quad (4b)$$

where γ_{Fe}^{gt} is an activity coefficient. Equation 3 can then be written with the compositionally dependent term K_D and a non-ideal term involving four activity coefficients:

$$\Delta G_{(1)}^0 = -RT \ln K_D - RT \ln \frac{\gamma_{MgSi_{1/2}O_2}^{ring} \gamma_{FeAl_{2/3}SiO_4}^{gt}}{\gamma_{MgAl_{2/3}SiO_4}^{gt} \gamma_{FeSi_{1/2}O_2}^{ring}} \quad (5)$$

In the simple case, both solid solutions can be treated as having symmetric deviations from ideal mixing, which for garnet can be described by:

$$RT \ln \gamma_{Fe}^{gt} = W_{FeMg}^{gt} (1 - X_{Fe}^{gt})^2 \quad (6a)$$

$$RT \ln \gamma_{Mg}^{gt} = W_{FeMg}^{gt} (1 - X_{Mg}^{gt})^2 \quad (6c)$$

where W_{FeMg}^{gt} is a Margules interaction parameter that describes the interaction energy between Fe^{2+} and Mg^{2+} cations in the garnet solid solution. Many partitioning studies have indicated that Fe^{2+}-Mg mixing in silicate and oxide solid solutions, including garnet, olivine, pyroxene, ringwoodite, and other spinel solid solutions, is described well by such symmetric models (O'Neill and Wood 1979; O'Neill and Wall 1988; Hackler and Wood 1989; Wiser and Wood 1991; von Seckendorff and O'Neill 1993; Frost et al. 2001). If asymmetry exists, therefore, it must be small and below the resolution of most data sets, particularly when correct uncertainties are assigned to the observations.

By using two symmetric interaction parameters to describe both solid solutions, Equation 3 becomes:

$$\Delta G_{(1)}^0 = -RT \ln K_D + W_{FeMg}^{gt} (2 X_{Fe}^{gt} - 1) + W_{FeMg}^{ring} (1 - 2 X_{Fe}^{ring}) \quad (7)$$

This equation can be fit to partitioning data using a non-linear least-squares algorithm to determine the two interaction parameters and $\Delta G_{(1)}^0$. However, as has been shown by many workers, values for the two interaction parameters are highly correlated and a range of values can still fit the correctly weighted data (O'Neill and Wood 1979; Hackler and Wood 1989; Wiser and Wood 1991; von Seckendorff and O'Neill 1993). Using cation-exchange data between two solid solutions enables only the difference between the interaction parameters (i.e., $W_{FeMg}^{gt} - W_{FeMg}^{ring}$) to be refined precisely. To determine the interaction parameter for one of the solid solutions, the interaction parameter for the other solid solution must first be known. In this study, the Fe-Mg partitioning between three solid solutions (garnet, ringwoodite, and magnesiowüstite) has been measured at high pressure and temperature. By measuring the partitioning among all three possible exchange reactions, more robust constraints can be placed on the individual interaction parameters for each solid solution.

The interaction parameters may also vary as a function of pressure and temperature according to:

$$W = W_U - TW_s + PW_V \quad (8)$$

Several studies have indicated that the temperature dependence of the interaction parameters for pyrope-almandine garnet, olivine, and ringwoodite may be ignored (O'Neill and Wood 1979; Frost et al. 2001), within the precision and temperature range of most data sets. Values of W_V can be determined from the excess volume of mixing, which for the pyrope-almandine garnet and ringwoodite solid solutions, are considered to be zero (Geiger and Feenstra 1997; Akaogi 1989).

EXPERIMENTAL PROCEDURE

Garnet and olivine solid solutions were prepared from reagent grade Fe_2O_3, MgO, Al_2O_3, and SiO_2. Pyrope-almandine compositions with Fe/(Fe + Mg) ratios of 0.05, 0.15, 0.4, 0.6, and 0.8, and olivine compositions with Fe/(Fe + Mg) ratios of 0.05, 0.1, 0.4, 0.6, and 0.8, were made by grinding the oxides together under alcohol. Pressed pellets of these mixtures were then reduced in a gas mixing CO-CO_2 furnace between 1200–1300 °C at an f_{O_2} 1 log unit above the iron-wüstite oxygen buffer. Recovered samples were then reground and reduced a second time. The pyrope-almandine powders were then converted to garnet using a 1/2-inch piston-cylinder apparatus at 2.5 GPa and 1250 °C using Fe capsules with a run duration of 1 day. Garnet and olivine solid solutions in the molar ratio of 5:1 were then ground together with an additional 20 wt% metallic Fe to produce the starting compositions shown in Table 1. Compositions of both solid solutions were chosen such that they would approach the suspected equilibrium composition from both higher and lower initial Fe contents. A pyrolite peridotite glass was prepared from oxides and carbonates that were reduced in a gas-mixing furnace and then melted in a graphite capsule at 1700 °C using an induction furnace with a controlled atmosphere. Rapid quenching produced a glass with some olivine crystallization. The glass was reground and combined with 20 wt% Fe metal.

Experiments were performed in a split-cylinder multianvil press using 10/5 (octahedral edge length/truncation edge length) octahedral sample assemblies and 32 mm Toshiba tungsten carbide cubes. The pressure calibration for this assembly has been reported previously (Frost et al. 2001). Multi-chamber capsules of Fe and Al_2O_3 were used such that 6 to 8 different compositions could be equilibrated in a single experiment. Al_2O_3 capsules were made from discs of 4-bore thermocouple ceramic with 300 μm sample holes. Up to 2 disks were placed inside a single outer molybdenum foil capsule with 0.1 mm disks of dense Al_2O_3 in between and top and bottom. $LaCrO_3$ heaters were employed with W3%Re/W25%Re thermocouple. The distance between the thermocouple and the samples did not exceed 0.5 mm. The temperature difference between the thermocouple and the measured surface of the samples was estimated to be on the order of 50°. Run times varied from 10 hours to two weeks. Experimental conditions are given in Table 2. Recovered charges were analyzed using Raman spectroscopy to determine the phases present and an electron microprobe was used to analyze phase compositions. Electron microprobe standards used were andradite for Si, enstatite glass for Mg, spinel for Al, and Fe metal.

TABLE 1. Starting compositions

	Garnet Fe/(Fe + Mg)	Olivine Fe/(Fe + Mg)	K_D
AB	0.05	0.1	0.47
AC	0.05	0.05	1.0
A	0.15	0.1	1.59
B	0.15	0.4	0.26
C	0.4	0.1	6.0
D	0.4	0.4	1.0
E	0.6	0.4	2.25
F	0.4	0.6	0.44
G	0.6	0.8	0.38
H	0.8	0.8	1.0

RESULTS

Pyrope-almandine

The run products in experiments where pyrope-almandine garnet was investigated consisted of garnet and either ringwoodite, wadsleyite, or olivine crystals of approximately 10–20 μm in diameter. In several runs, magnesiowüstite was also formed. In all experiments, metallic Fe remained dispersed throughout the samples after the experiment. Where Al_2O_3 capsules were employed, very minor reaction rims adjacent to the capsule wall were observed where the $(Mg,Fe)_2SiO_4$ phase had reacted to produce garnet. These rims were generally no more than 20–30 μm in width. Many garnet grains were zoned with unreacted cores of compositions close to the starting garnet composition. This zoning was found even in experiments performed at 1400 °C for over two weeks. Grains of the $(Mg,Fe)_2SiO_4$ phases displayed no zonation. Garnet microprobe analyses (reported in Table 3) were made on rims closest to coexisting $(Mg,Fe)_2SiO_4$ grains or on grains <10 μm in diameter, which generally displayed no zonation. Between 10 and 20 pairs of analyses were collected from each composition.

Some variation in the garnet Al_2O_3 content occurred in the experimental products. The Al contents in atoms per $Mg_3Al_2Si_3O_{12}$ formula unit ranged between 1.6 and 2 within some samples. As no coupling was observed between the Al content and the Fe/(Fe + Mg) ratio in this range of compositions, it was assumed that small majorite components do not

TABLE 2. Experimental run conditions

Run	Capsule	T (°C)	Pressure (GPa)	Starting materials	Time (days)
H1554	Fe	1400	18.0	Py-Alm + Ol, Pyro	0.6
H1555	Fe	1400	15.0	Py-Alm + Ol, Pyro	0.4
H1556	Fe	1400	13.0	Py-Alm + Ol, Pyro	0.4
V170	Al_2O_3	1400	19.0	Py-Alm + Ol, Pyro	16.0
H1582	Al_2O_3	1400	18.0	Py-Alm + Ol, Pyro	0.6
V171	Al_2O_3	1500	18.0	Py-Alm + Ol, Pyro	5.0
S2773	Fe	1400	9.5	Py-Alm + Ol, Pyro	0.6
H1572	Fe	1400	18.0	Gr, Mj + Ol, Pyro	0.6
V172	Al_2O_3	1400	13.0	Py-Alm + Ol, Pyro	5.0
V175	Al_2O_3	1400	14.0	Py-Alm + Ol, Pyro	10.0
V179	Al_2O_3	1400	18.0	Gr, Mj + Ol, Pyro	11.0
V191	Al_2O_3	1400	14.0	Ol + Mw, Pyro	1.0
V193	Al_2O_3	1400	18.0	Py-Alm + Mw, Pyro	6.0
V197	Al_2O_3	1700	18.0	Py-Alm + Ol, Pyro	2.0

Notes: Py-Alm + Ol refers to starting materials of pyrope-almandine garnet plus olivine as given in Table 1. Pyro refers to pyrolite peridotite glass staring material. Gr, Mj + Ol refers to grossular and majorite rich garnet experiments.

significantly affect the Fe-Mg partitioning relations. At higher temperatures (>1400 °C) and above 10 GPa, garnet becomes significantly more majoritic because $(Mg,Fe)_2SiO_4$ phases react to produce majorite and magnesiowüstite through a reaction which, in terms of end-members, can be considered as:

$$\underset{\text{ringwoodite}}{Mg_2SiO_4} = \underset{\text{majorite}}{MgSiO_3} + \underset{\text{oxide}}{MgO} \quad (9)$$

An experiment performed at 18 GPa and 1700 °C, for example, produced only majoritic garnet and magnesiowüstite because ringwoodite had broken down completely.

Figure 1 shows the distribution coefficient K_D, as defined in Equation 2, between garnet and the 3 polymorphs ringwoodite, wadsleyite, and olivine plotted against the garnet Fe/(Fe + Mg) ratio for experiments performed between 9 and 19 GPa and 1400–1500 °C. Error bars are propagated from 1σ uncertainties in the garnet and $(Mg,Fe)_2SiO_4$ phase compositions from the microprobe analyses. For ringwoodite, K_D varies as a function of composition, which implies that mixing in at least one of the solid solutions is non-ideal. Although a complete set of reversals was not made at each pressure for garnet-ringwoodite experiments, there appears to be little pressure dependence to the partitioning over this 6 GPa range, within the uncertainty of the data.

The data coverage for wadsleyite-garnet partitioning is quite limited because wadsleyite becomes unstable above a Fe/(Fe + Mg) ratio of approximately 0.3. Although the results appear to be consistent with a very weak compositional dependence for the garnet-wadsleyite K_D, the uncertainties would still allow K_D to have a significant positive or negative compositional dependence.

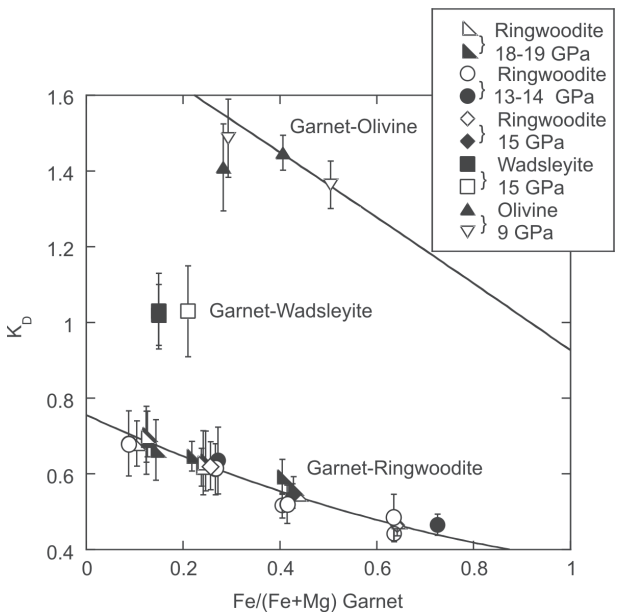

FIGURE 1. Fe-Mg partitioning between pyrope-almandine garnet and olivine, garnet-wadsleyite, and garnet-ringwoodite collected at pressures between 9.5 and 19 GPa and at 1400 °C. K_D is defined as $(Fe/Mg)_{gt}/(Fe/Mg)_{ol}$ as in Equation 2. The curve through the garnet-olivine data is calculated from the model of O'Neill and Wood (1979) at 9.5 GPa and 1400 °C. The curve through the garnet-ringwoodite data is a best fit to these results. Open symbols approached equilibrium from initially lower starting K_D values and closed symbols approached from the high K_D direction.

The results for olivine were also collected over too narrow a compositional range for these data to be useful in their own right for refining thermodynamic properties, however, these data have been compared in Figure 1 with an extrapolation of the model by O'Neill and Wood (1979) to 9.5 GPa and 1400 °C. The data and model agree remarkably well considering the model was derived from data collected at 3 GPa.

Pyrolite composition

Experiments using a pyrolite peridotite composition were performed using a pre-prepared glassy sample, which had partially crystallized olivine. Between 14 and 19 GPa, the glass portion of this composition crystallized to majoritic garnet and the olivine transformed to either ringwoodite or wadsleyite. Analyses of these phases are reported in Table 4. Mass-balance calculations revealed the composition to comprise 59 vol% $(Mg,Fe)_2SiO_4$ and 41% majoritic garnet. In experiments from 14 GPa, the presence of minor amounts of clinopyroxene was detected using Raman spectroscopy but this phase was too fine grained for analysis with the microprobe. The amount of pyroxene crystallizing at these conditions is likely to be below 10%. Below 14 GPa, pyroxene became more abundant and areas of the sample that had originally been glass in the starting mixture crystallized to a sub-micrometer, fine-grained assemblage of clinopyroxene and garnet. Microprobe analyses of this fine-grained mixture were unreliable and are therefore not reported.

Mass-balance calculations showed that in experiments performed in multi-chamber Fe capsules, as much as 8 wt% FeO was added to the bulk composition from oxidation of metallic Fe. For experiments performed in Al_2O_3 capsules, on average, only 1.5 wt% additional FeO was formed by oxidation. This difference most likely arises because Fe capsules are permeable to oxygen at these conditions. All capsules used contained multiple sample chambers where other pyrope-almandine starting compositions were placed, with a variety of bulk Fe/(Fe + Mg) ratios. FeO-rich bulk compositions in equilibrium with metallic Fe impose a higher local f_{O_2} than more MgO-rich compositions. In Fe capsules, however, all the sample chambers are connected via oxygen diffusion through the capsule walls. As a consequence, metallic Fe in more MgO-rich compositions tends to be oxidized, whereas FeO-rich compositions tend to precipitate metallic Fe. All samples in the multi-chamber metal capsules, therefore, shift in composition to approach a single f_{O_2} and FeO content. As peridotite compositions were less FeO-rich than some of the other staring compositions, Fe was oxidized in these samples thus increasing the bulk FeO content. The change in bulk FeO content as a result of this redox process seems to occur at a slower rate than Fe-Mg diffusion, such that it does not affect the partitioning results. Different compositions run in multi-chamber metal capsules for many days do tend to converge, however, to a single Fe/(Fe + Mg) ratio.

In the pressure interval 14–19 GPa, the garnets produced in

TABLE 3. Pyrope-almandine garnet partitioning results

	Phase	Fe	Al	Si	Mg	Cation total	Fe/ (Fe + Mg)
H1554	18GPa 1400 °C						
A	Gt	0.42(3)	1.94(4)	3.00(1)	2.66(4)	8.025	0.144(9)
	Ring	1.20(3)	0.05(5)	2.98(1)	4.75(9)	8.992	0.202(7)
	Oxide	3.87	0.035	0.049	7.978	11.93	0.327
B	Gt	0.76(5)	1.8(1)	3.08(8)	2.41(7)	8.033	0.241(13)
	Ring	2.05(7)	0.03(2)	2.9(2)	4.1(3)	9.071	0.335(12)
	Oxide	6.969	0	0	5.031	12.00	0.581
E	Gt	1.28(4)	1.85(6)	3.02(2)	1.89(5)	8.051	0.405(11)
	Ring	3.10(8)	0.04(6)	2.98(2)	2.87(6)	8.996	0.534(7)
H1555	15 GPa 1400 °C						
B	Gt	0.79(2)	1.9(1)	3.04(5)	2.29(7)	8.012	0.257(9)
	Ring	2.13(7)	0.02(1)	2.99(1)	3.85(7)	8.996	0.357(11)
	Oxide	7.03(1)	0.03(1)	0.047(0)	4.836(8)	11.94	0.592(1)
E	Gt	1.34(5)	1.89(6)	3.03(2)	1.78(3)	8.032	0.426(10)
	Ring	3.44(5)	0.03(6)	3.00(1)	2.51(4)	8.984	0.578(4)
G	Gt	2.01(6)	1.90(5)	3.01(2)	1.12(2)	8.037	0.642(10)
	Ring	4.74(2)	0.01(6)	3.00(1)	1.23(2)	8.989	0.794(3)
H1556	15 GPa 1400 °C						
A	Gt	0.47(3)	1.96(2)	2.96(1)	2.68(3)	8.063	0.149(10)
	Wad	0.90(2)	0.06(8)	2.90(2)	5.21(4)	9.072	0.147(3)
B	Gt	0.71(3)	1.87(6)	2.98(2)	2.52(7)	8.086	0.214(14)
	Wad	1.28(9)	0.04(6)	2.906(6)	4.84(7)	9.072	0.209(14)
E	Gt	1.99(3)	1.92(5)	2.98(2)	1.15(3)	8.055	0.635(7)
	Ring	4.75(7)	0.000	2.96(1)	1.3(1)	9.040	0.782(16)
G	Gt	1.29(5)	1.87(8)	2.99(3)	1.91(5)	8.072	0.404(10)
	Ring	3.44(6)	0.03(3)	2.94(1)	2.62(15)	9.041	0.568(5)
V170	19 GPa 1400 °C						
A	Gt	0.38(2)	1.99(2)	3.00(2)	2.63(2)	8.004	0.126(6)
	Ring	1.02(2)	0.019(7)	2.97(1)	5.010(9)	9.023	0.17(4)
AB	Gt	0.31(3)	1.97(2)	3.02(1)	2.69(3)	7.994	0.104(9)
	Ring	0.92(5)	0.02(1)	2.98(9)	5.09(9)	9.011	0.154(7)
AC	Gt	0.38(3)	1.89(4)	3.04(2)	2.70(1)	8.013	0.124(9)
	Ring	1.03(4)	0.018(5)	2.961(7)	5.02(3)	9.03	0.170(6)
B	Gt	0.73(3)	1.86(8)	3.07(4)	2.33(4)	7.996	0.238(10)
	Ring	1.99(3)	0.02(1)	3.02(1)	3.95(2)	8.975	0.336(4)
F	Gt	1.53	1.378	3.21	1.98	8.102	0.437
	Ring	3.49	0	3.013	2.466	8.983	0.586
G	Gt	1.97(3)	1.90(6)	3.04(2)	1.10(2)	8.013	0.641(2)
	Ring	4.71(2)	0.008(2)	3.02(1)	1.25(1)	8.98	0.791(2)
E	Gt	1.31(5)	1.91(2)	3.03(1)	1.76(2)	8.013	0.428(10)
	Ring	3.4(6)	0.02(5)	3.00(2)	2.6(2)	8.99	0.569(3)
H1582	18 GPa 1400 °C						
A	Gt	0.41(5)	1.91(4)	2.98(2)	2.75(4)	8.061	0.135(10)
	Ring	1.09(5)	0.03(2)	2.92(3)	5.04(5)	9.071	0.178(8)
B	Gt	0.76(6)	1.8(3)	3.0(2)	2.5(1)	8.083	0.239(10)
	Ring	2.07(2)	0.03(3)	2.94(2)	4.00(5)	9.046	0.341(4)
E	Gt	1.494	1.51	3.16	1.918	8.085	0.438
	Ring	3.58(3)	0(0)	2.95(8)	2.51(2)	9.047	0.588(4)
F	Gt	1.27(5)	1.91(5)	2.985(9)	1.88(8)	8.058	0.403(2)
	Ring	3.37(2)	0.004(6)	2.93(2)	2.75(4)	9.065	0.551(5)
V171	18 GPa 1500 °C						
A	Gt	0.38(1)	1.91(6)	3.04(4)	2.67(2)	8.002	0.124(3)
	Ring	1.05(1)	0.029(8)	2.98(3)	4.95(5)	9.008	0.175(2)
	Wad	0.72(4)	0.046(6)	2.98(1)	5.24(1)	8.993	0.121(1)
	Oxide	3.00(5)	0.04(1)	0.06(7)	8.8(1)	11.92	0.254(1)
S2773	9.5 GPa 1400 °C						
E	Gt	1.60(44)	1.9(1)	2.97(7)	1.57(6)	8.068	0.505(9)
	Ol	2.58(7)	0.02(5)	2.96(1)	3.46(9)	9.027	0.428(12)
B	Gt	0.89(5)	1.9(1)	3.00(5)	2.24(6)	8.046	0.283(14)
	Ol	1.32(9)	0.009(8)	2.97(9)	4.72(9)	9.022	0.219(16)
F	Gt	1.3(1)	1.8(2)	3.03(2)	1.9(2)	8.076	0.406(8)
	Ol	1.9(2)	0.003(3)	2.9(3)	4.1(4)	9.024	0.321(7)
G	gt	1.9(1)	2.0(3)	2.9(2)	1.09(8)	8.03	0.639(16)
	Ring	4.92	0	2.949	1.184	9.051	0.806
A	Gt	0.92(4)	1.87	3.02(5)	2.22(6)	8.041	0.293(13)
	Ol	1.31(8)	0.011	2.973(8)	4.72(9)	9.021	0.218(14)

Notes: 1 sigma uncertainties shown in brackets are in terms of least units cited.

TABLE 3. —*Continued*

V175	14 GPa 1400 °C						
A	Gt	0.45(4)	1.98(2)	2.97(2)	2.62(4)	8.036	0.148(13)
	Wad	0.86(2)	0.059(2)	2.95(1)	5.14(2)	9.017	0.144(3)
D	Gt	0.87(5)	1.9(1)	2.96(6)	2.39(9)	8.102	0.267(17)
	Ring	2.26(5)	0.03(6)	2.94(1)	3.80(6)	9.042	0.373(5)
B	Gt	0.86(7)	1.9(1)	3.00(4)	2.30(9)	8.053	0.272(21)
	Ring	2.23(4)	0.009(3)	2.98(1)	3.79(3)	9.012	0.370(6)
H	Gt	2.27(4)	1.93(1)	2.99(1)	0.83(1)	8.036	0.733(6)
	Ring	5.08(3)	0.008(2)	2.99(1)	0.93(1)	9.007	0.846(3)
G	Gt	1.95(2)	1.957(9)	3	1.12(2)	8.022	0.636(6)
	Ring	4.80(7)	0.008(2)	2.99(3)	1.217(9)	9.011	0.798(3)
F	Gt	1.33(7)	1.95(1)	2.92(2)	1.88(5)	8.1	0.42(2)
	Ring	3.55(3)	0.014(1)	2.91(1)	2.60(2)	9.083	0.577(4)
V179	18 GPa 1400 °C						
D	Gt	0.79(5)	1.84(8)	3.02(4)	2.41(5)	8.059	0.24(1)
	Ring	2.02(3)	0.1(1)	2.98(3)	3.9(1)	8.981	0.34(1)
B	Gt	0.68(3)	1.90(5)	3.01(2)	2.44(3)	8.037	0.218(7)
	Ring	1.80(3)	0.024(9)	2.98(2)	4.18(2)	9	0.301(4)
A	Gt	0.38(2)	1.95(17)	2.99(6)	2.69(2)	8.025	0.124(6)
	Ring	1.01(4)	0.031(2)	2.99(2)	4.95(4)	8.988	0.169(6)

Notes: 1 sigma uncertainties shown in brackets are in terms of least units cited.

the peridotite composition had Al concentrations that were half way between pyrope and majorite end-members, i.e., 1 Al atom per formula unit. Calcium contents were approximately 0.6 per formula unit. Figure 2 shows the Fe-Mg distribution coefficient between ringwoodite and garnet within the peridotitic composition. There is a slightly larger dependence of K_D on the garnet Fe/(Fe + Ca + Mg) ratio in the more complex peridotite system when compared with the results for pyrope-almandine garnet at the same conditions. This result is in general agreement with previous studies that have also crystallized majoritic garnet of similar CaO and Al_2O_3 contents. Over the range of Fe/(Fe + Ca + Mg) ratio investigated, however, the difference in K_D between complex and simple garnets is very small and the two sets of data are consistent with each other within the error bars. Data points of Wood (2000) and Nishihara and Takahashi (2001) that display much higher K_D also have large or unreported uncertainties and may also be in reasonable agreement with both the complex and simple garnet data reported here.

Results of wadsleyite-garnet partitioning in the peridotite system are shown in Figure 3. Although the range of Fe contents investigated is small, the data from 1400 and 1700 °C display a very similar range in K_D as the pyrope-almandine results. Results at 1700 °C indicate that increasing the temperature lowers K_D for a given Fe content but this effect is also relatively small. Previous results of Irifune and Isshiki (1998) and Nishihara and Takahashi (2001) collected at similar pressures and temperatures display a considerable range of values, which are difficult to bring into agreement with the results of this study. A possible difference is the presence Fe^{3+} in these previous studies, as the oxygen fugacity was not buffered.

Above 15 GPa in the pyrolite peridotite composition studied here, majoritic garnet was the only Al- and Ca-bearing phase present, even after experiments run for 16 days. Fe-Mg partitioning between the garnet and olivine polymorph is therefore the only exchange reaction taking place and the only reaction for which equilibrium needs to be demonstrated. The starting composition contained olivine and glass with a starting $K_D^{Fe\text{-}Mg}$ >7. Although equilibrium partitioning was only approached

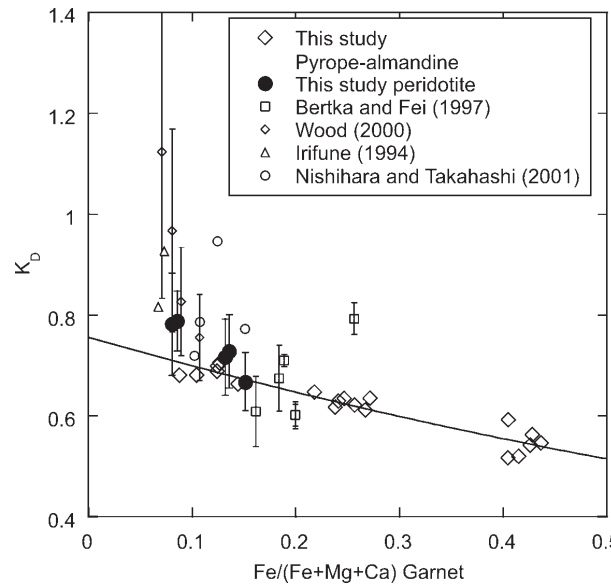

FIGURE 2. Fe-Mg partitioning results between garnet and ringwoodite in a peridotite composition at 1400 °C display a slightly steeper trend in comparison to results from pyrope-almandine garnet partitioning. The two sets of data are, however, consistent with each other within the experimental error. At these conditions, garnet in the peridotite composition has 1 Al and 0.6 Ca atoms per formula unit. Several previous studies where peridotite compositions have been used are also shown. K_D is defined as in Equation 2.

from one direction, the Fe contents of both phases changed significantly during the course of even relatively short experiments. Experiments run for ten hours in the ringwoodite stability field at 1400 °C, for example, showed similar large changes in K_D as experiments run for two weeks. Similarly, in the wadsleyite stability field, an experiment run for one day displayed almost identical results to one left for 5 days. Therefore, it is considered that Fe-Mg equilibrium was achieved in these compositions more rapidly than the shortest experiments,

TABLE 4. Pyrolite peridotite results

	Phase	Fe	Al	Ca	Si	Mg	Cation total	Fe/ (Fe + Mg + Ca)
pyrolite		0.49	0.38	0.27	3.27	4.12		0.106
H1554	18 GPa 1400 °C							
	Gt	0.45(3)	0.97(6)	0.67(5)	3.57(3)	2.29(7)	7.949	0.132(7)
	Ring	1.28(6)	0.02(2)	0.02(2)	3.00(2)	4.66(8)	8.987	0.22(1)
H 1555	15 GPa 1400 °C							
	Gt	0.51(3)	0.9(1)	0.72(4)	3.59(5)	2.13(9)	7.923	0.151(9)
	Ring	1.55(6)	0.04(6)	0.03(4)	3.00(3)	4.4(2)	8.977	0.263(8)
H1572	18 GPa 1400 °C							
	Gt	0.45(2)	0.94(7)	0.74(6)	3.65(5)	2.1(1)	7.882	0.136(8)
	Ring	1.35(5)	0.008(7)	0.012(7)	3.00(1)	4.63(5)	8.999	0.227(9)
V170	19 GPa 1400 °C							
	Gt	0.29(2)	0.88(7)	0.65(9)	3.60(4)	2.5(1)	7.955	0.084(4)
	Ring	0.77(2)	0.015(2)	0.01(1)	2.98(2)	5.23(5)	9.013	0.129(2)
V179	18 GPa 1400 °C							
	Gt	0.29(2)	1.00(5)	0.64(3)	3.47(2)	2.62(7)	8.026	0.081(7)
	Ring	0.73(4)	0.012(7)	0.005(3)	3.02(1)	5.22(5)	8.979	0.123(8)
V175	14 GPa 1400 °C							
	Gt	0.35(1)	0.94(3)	0.68(1)	3.59(2)	2.38(2)	7.941	0.103(3)
	Wad	0.76(2)	0.013(3)	0.006(1)	2.99(1)	5.23(1)	9.002	0.127(3)
V193	18 GPa 1400 °C							
	Gt	0.41(3)	0.90(7)	0.61(3)	3.54(4)	2.5(1)	8.01	0.114(8)
	Wad	0.74(2)	0.020(1)	0.00(0)	2.99(1)	5.26(3)	9.00	0.123(3)
V191	14 GPa 1400 °C							
	Gt	0.39(2)	0.96(7)	0.66(8)	3.58(2)	2.3(1)	7.94	0.114(4)
	Wad	0.77(3)	0.01(0)	0.01(1)	3.01(1)	5.19(3)	8.99	0.129(4)
V197	18 GPa 1700 °C							
	Gt	0.40(1)	0.91(7)	0.37(4)	3.54(3)	2.79(2)	8.01	0.112(3)
	Wad	0.82(2)	0.06(0)	0.00(0)	2.97(1)	5.15(1)	9.00	0.137(2)
	Oxide	3.20(2)	0.070(5)	0.007(1)	0.011(1)	8.64(1)	11.95	0.27(15)
H1556	13 GPa 1400 °C							
	Gt	0.54(2)	0.91(6)	0.5(1)	3.56(4)	2.47(7)	7.98	0.154(4)
	Wad	1.13(2)	0.03(2)	0.01(1)	2.99(1)	4.82(5)	8.988	0.190(3)
	Olivine	0.66(2)	0.012(5)	0.011(2)	2.98(1)	5.35(4)	9.011	0.110(4)

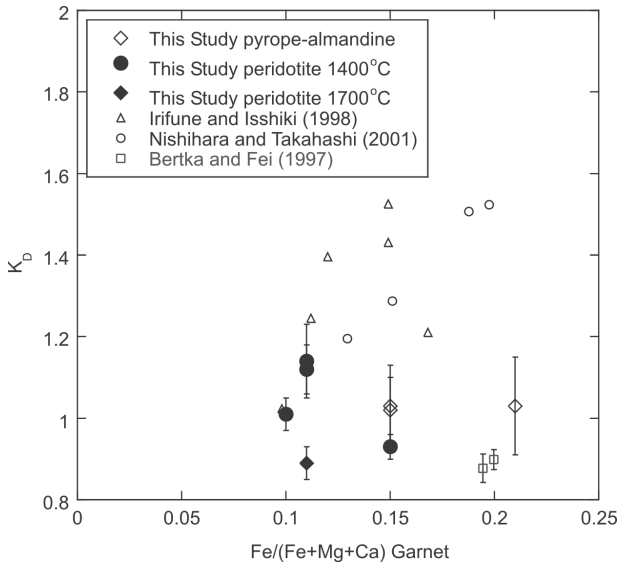

FIGURE 3. Results of wadsleyite-garnet partitioning in a peridotite composition at 1400 °C are compared with partitioning experiments between pyrope-almandine garnet and wadsleyite. Results from several previous studies where peridotite compositions have been used also are shown.

which were run for ten hours. This result is in contrast to experiments performed on pyrope-almandine compositions, which showed significant garnet zonation even after several weeks. The use of glass as a starting material in the peridotite experiments may have resulted in a faster approach to equilibrium than for pyrope-almandine garnets. On the other hand, it is also possible that Fe-Mg diffusion is faster in majoritic garnets.

Grossular and majorite

In the pyrolite peridotite composition, the results for garnet-ringwoodite Fe-Mg partitioning show a slightly stronger compositional dependence than partitioning results on the pyrope-almandine join but the two sets of data are, within error, consistent with each other. In Figure 4, the influences of both grossular and majorite components have been investigated separately to understand the absence of a combined effect on the peridotite partitioning. Starting compositions were pre-synthesized Ca-bearing garnets and Al-bearing enstatites. Results are given in Table 5. For Ca-bearing garnets, the Fe-Mg partition coefficient K_D increases with increasing Ca content in line with similar observations made during a study on olivine-garnet Fe-Mg partitioning (O'Neill and Wood 1979). This increase results from Fe-Ca interactions being energetically more favorable than Mg-Ca interactions in garnet. The magnitude of the effect on K_D expected due to Ca can be calculated using the model of O'Neill and Wood (1979). This model predicts a slightly smaller influence than observed experimentally but the model's predictions are well within the experimental uncertainties. Garnets formed in the peridotitic composition at these conditions contain around 0.6 Ca atoms per formula unit and would therefore be expected to plot at higher K_D than simple pyrope-almandine garnets. The actual peridotite trend is, however, lower than predicted for such a Ca content.

Results from majoritic garnet-ringwoodite partitioning experiments where garnets contained 0.5 Al atoms per formula

unit plot slightly below the trend for pyrope-almandine garnets. The partitioning trend for peridotite may therefore result from a combination of influences from majorite and grossular components that affect K_D in opposite directions. For ranges of Fe/(Fe + Mg + Ca) ratio between 0.12 and 0.2, these influences apparently cancel out and the values for K_D in the peridotite composition are, within error, identical to those for pyrope-almandine garnets.

Activity-composition relations for garnet, ringwoodite and magnesiowüstite

The garnet-ringwoodite partitioning data can be used to refine thermodynamic parameters for the non-ideality of Fe and Mg mixing in both pyrope-almandine and ringwoodite solid solutions. By globally fitting these data with results from Fe-Mg partitioning between garnet and magnesiowüstite and between ringwoodite and magnesiowüstite (Frost et al. 2001), however, allows more robust constraints to be placed on the refined thermodynamic parameters and those of magnesiowüstite can also be determined. As shown in Figure 5, these three data sets were globally fit with a weighted nonlinear least-squares regression using Equation 7. At 18 GPa and 1400 °C, this approach still results in ranges of values for each interaction parameter that can fit the correctly weighted data. This is because the interaction parameters are highly correlated due to the form of Equation 7. These ranges are 11–14 kJ/mol for magnesiowüstite, 2.0–5.0 kJ/mol for ringwoodite, and –2.0–2.0 kJ/mol for garnet. However, over these ranges of values, the differences between the interaction parameters are constrained very well. These are $W^{mw}_{FeMg} - W^{ring}_{FeMg} = 8.8(2)$ kJ/

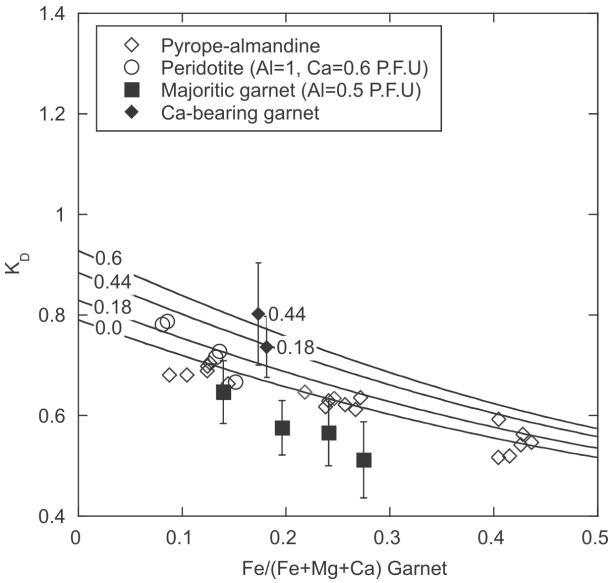

FIGURE 4. The effects of grossular and majorite garnet components on the Fe-Mg partitioning between garnet and ringwoodite are examined individually at 1400 °C. Data for Ca-bearing garnets with no majorite component are shown with the Ca content in atoms per formula unit (per formula unit (pfu) normalized to 12 oxygen atoms) to the right of each data point. The variation of K_D with Ca content calculated using the model of O'Neill and Wood (1979) for garnet is shown contoured for the Ca content in atoms pfu Experiments on Ca-free majoritc garnets with Al = 0.5 atom pfu are also shown.

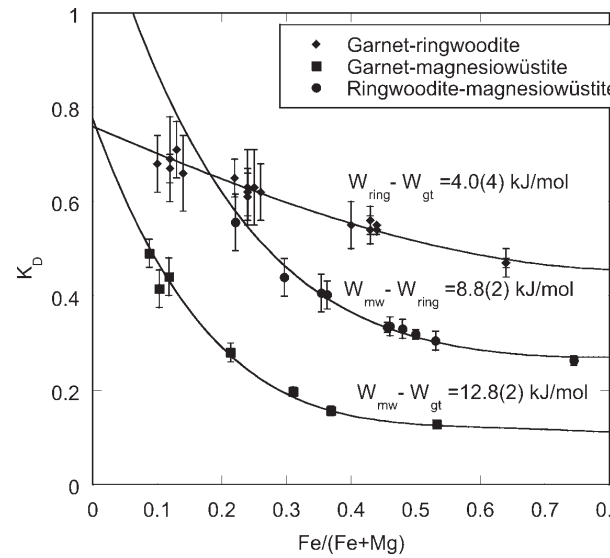

FIGURE 5. Garnet-ringwoodite, garnet-magnesiowüstite, and ringwoodite-magnesiowüstite (Frost et al. 2001) partitioning data are used to refine symmetric Margules interaction parameters for Fe-Mg mixing in these solid solutions at 18 GPa and 1400 °C. All pyrope-almandine garnet-ringwoodite data collected between 14 and 19 GPa were used in the refinement because no influence of pressure was observed in this range. Globally fitting these data provides good estimates for the differences in symmetric interaction parameters. These differences are then solved simultaneously to give individual interaction parameters.

TABLE 5. Effects of grossular and majorite garnet components

	Phase	Fe	Al	Ca	Si	Mg	Total	Fe/ (Fe + Mg)
V179	18GPa 1400°C							
Ca1	Gt	0.42(4)	1.8(1)	0.19(4)	3.05(5)	2.59(6)	8.05	0.132(11)
	Ring	1.03(2)	0.03(5)		3.00(1)	4.9(1)	8.978	0.173(6)
Ca2	Gt	0.38(3)	1.94(3)	0.44(5)	2.99(1)	2.28(7)	8.041	0.123(12)
	Ring	1.08(1)	0.030(9)		2.99(1)	4.88(2)	8.99	0.181(2)
Maj1	Gt	0.47(3)	0.60(8)	0.012(5)	3.65(4)	3.31(5)	8.045	0.123(6)
	Ring	1.17(3)	0.017(9)		3.00(1)	4.79(4)	8.988	0.196(5)
Maj2	Gt	0.37(3)	0.55(5)	0.026(9)	3.63(6)	3.51(4)	8.092	0.095(6)
	Ring	0.83(2)	0.028(9)		3.00(1)	5.13(2)	8.986	0.140(3)
H1572	18 GPa 1400°C							
Maj3	Gt	0.58(3)	0.49(4)	0.00(0)	3.72(3)	3.24(4)	8.034	0.152(7)
	Ring	1.45(6)	0.003(4)	0.00(0)	2.983(9)	4.58(6)	9.015	0.241(11)
Maj4	Gt	0.62(4)	0.53(7)	0.005(5)	3.68(3)	3.21(6)	8.053	0.162(13)
	Ring	1.65(6)	0.012(3)		2.97(1)	4.37(4)	9.019	0.275(9)

mol, $W^{mw}_{FeMg} - W^{gt}_{FeMg}$ = 12.8(5) kJ/mol, and $W^{ring}_{FeMg} - W^{gt}_{FeMg}$ = 4.0(4) kJ/mol. These differences can then be solved simultaneously to give the individual interaction parameters W^{mw}_{FeMg} = 13.2(5) kJ/mol, W^{ring}_{FeMg} = 4.4(3) kJ/mol, and W^{gt}_{FeMg} = 0.3(4) kJ/mol on a single-site basis. The corresponding values for the free-energy changes of the cation exchange reactions are 7.8(3) kJ/mol for garnet-ringwoodite, 18.1(3) kJ/mol for garnet-magnesiowüstite, and 9.3(2) kJ/mol for ringwoodite-magnesiowüstite.

DISCUSSION

In many previous studies on Fe-Mg partitioning, cation exchange between two solid solutions has been measured and the activity-composition relations for one of these solid solutions have been determined using known thermodynamic mixing properties for the other solid solution. At one atmosphere, the Fe-Mg activity-composition relations for a solid solution can be determined precisely, independently of partitioning data, by studying the redox equilibria between the solid solution and metallic Fe. To extrapolate activity-composition relations to high pressure requires only knowledge of the excess volume of mixing. Magnesiowüstite is by far the most useful standard solid solution by which to extract Fe-Mg activity composition relations from partitioning data. Magnesiowüstite has precisely determined activity-composition relations at 1 bar, is stable over large pressure ranges, and coexists with a wide range of other phases. However, due to the increase in Fe^{3+} and non-stoichiometry in magnesiowüstite at high Fe/(Fe + Mg) ratios, the excess volume of mixing for MgO-"FeO" magnesiowüstite is difficult to determine precisely, which introduces a significant uncertainty into the high-pressure extrapolation of 1 bar activity-composition relations.

O'Neill et al. (2003) have recently used an electrochemical technique to determine precisely the activity-composition relations for the magnesiowüstite solid solution in equilibrium with metallic Fe at 1 bar. Their results take into account the Fe^{3+} concentration in magnesiowüstite and find the solid solution to be slightly asymmetric. These data also include the temperature dependence of W^{mw}_{FeMg} at 1 bar. Ignoring the relatively small contributions from the asymmetric term and the Fe^{3+} content, and extrapolating in temperature to 1400 °C, these data give a value for W^{mw}_{FeMg} at 1 bar of approximately 11 kJ/mol. By comparing this 1 bar value to the high-pressure determination made in this study provides an estimate for Wv^{mw}_{FeMg}, as defined in Equation 8, of 110 J/GPa.

Several previous determinations of W^{gt}_{FeMg} have been made using Fe-Mg partitioning data between garnet and olivine. O'Neill and Wood (1979) determined W^{gt}_{FeMg} to be 0.8 kJ/mol at 3 GPa, and Hackler and Wood (1989) obtained W^{gt}_{FeMg} = 1.6 kJ/mol at 0.95 GPa. In both of these previous studies, however, values for W^{oline}_{FeMg} of approximately 4.5 kJ/mol were used to refine the value of W^{gt}_{FeMg} from the partitioning data. O'Neill et al. (2003) have used their revised data on the magnesiowüstite solid-solution to reassess W^{oline}_{FeMg} using the magnesiowüstite-olivine partitioning data of Wiser and Wood (1991). The refined value of 2.57 kJ/mol for W^{oline}_{FeMg} is smaller than that used in the previous garnet-olivine partitioning studies but when applied to these data values for W^{gt}_{FeMg} of essentially zero are obtained. The spectroscopic study of Ballaran et al. (1999) also concluded that mixing was most likely ideal in pyrope-almandine garnets. The fact that W^{gt}_{FeMg} is close to zero at low pressure and at 18 GPa implies that Wv^{gt}_{FeMg} is also close to zero, which is in agreement with the excess molar volume measurements of Geiger and Fennestra (1997).

One of the principal reasons for studying Fe-Mg exchange between transition-zone minerals is to determine how the Fe/(Mg + Fe) ratios of individual minerals will vary as a function of depth in the mantle. Specifically, it is important to be able to calculate the Fe/(Mg + Fe) ratio of $(Mg,Fe)_2SiO_4$ polymorphs at conditions within the transition zone where these phases transform. As demonstrated by Irifune and Isshiki (1998), the presence of garnet and clinopyroxene at conditions applicable to the 410 km discontinuity results in an effective narrowing of the pressure interval over which the divariant transformation of olivine to wadsleyite takes place. The amount of Fe that is partitioned into garnet decreases across the phase transformation because the garnet-olivine K_D is substantially larger than the garnet-wadsleyite K_D. The Fe/(Mg + Fe) ratio of wadsleyite is consequently greater on the high-pressure side of the transformation than the Fe/(Mg + Fe) ratio of olivine on the low-pressure side. The increase in the wadsleyite Fe content means that it becomes stable at a lower pressure than in a garnet free system and the pressure interval of the transformation is narrowed. By using the partitioning data collected in this study, this effect can be calculated and the results compared with studies on whole-rock compositions such as that of Irifune and Isshiki (1998).

In Figure 6, the Fe-partitioning data collected for pyrope-

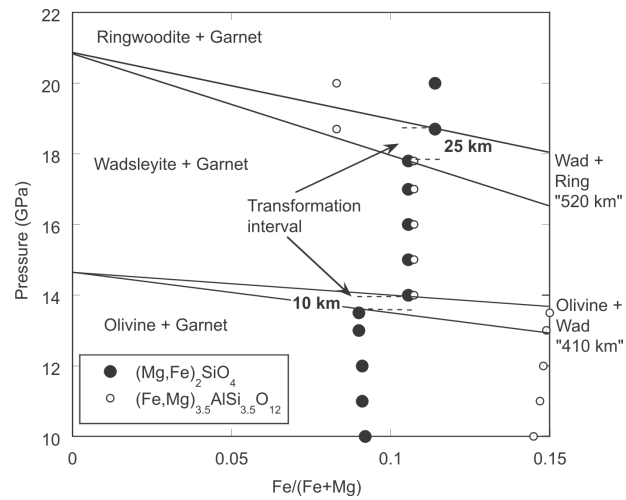

FIGURE 6. The change in Fe/(Fe + Mg) ratio of $(Fe,Mg)_2SiO_4$ polymorphs due to Fe-Mg partitioning between these phases and 40% garnet is calculated between 10 and 20 GPa at 1400 °C. The pressure intervals of the olivine to wadsleyite and wadsleyite to ringwoodite transformations in the Fe_2SiO_4-Mg_2SiO_4 system are indicated (Fei and Bertka 1999; Katsura and Ito 1989). The Fe/(Fe + Mg) ratio of the $(Fe,Mg)_2SiO_4$ phase is always higher on the high-pressure side of the transformation because Fe partitions out of garnet as each higher pressure $(Fe,Mg)_2SiO_4$ polymorph becomes stable. This results in a narrowing of the transformation pressure interval as indicated by the dashed lines.

almandine garnet, wadsleyite, and ringwoodite have been used to calculate the Fe/(Mg + Fe) ratios of these phases between 10 and 20 GPa for a typical peridotite Fe/(Mg + Fe) ratio. The model of O'Neill and Wood (1979), which satisfactorily described partitioning data collected in this study at 9.5 GPa, has been used to calculate the olivine and garnet Fe/(Mg + Fe) ratios. The olivine to wadsleyite transformation at 1400 °C determined by Fei and Bertka (1999), and the wadsleyite to ringwoodite transformation at 1600 °C by Katsura and Ito (1989), are also shown in Figure 6. The calculation considers peridotite to be made of 60% $(Mg,Fe)_2SiO_4$ and 40% $(Mg,Fe)_{3.5}AlSi_{3.5}O_{12}$ garnet. This is obviously a simplification because a peridotite composition not only contains clinopyroxene up to 15 GPa but garnet also contains grossular in addition to majorite components. The amount of clinopyroxene present at the 410 km discontinuity, however, is expected to be quite low (approximately 10 vol%). Moreover, because clinopyroxene is Fe-poor compared to garnet, its presence will have a slightly smaller effect in comparison to garnet in terms of narrowing the pressure interval of the transformation. The presence of grossular and majorite components in garnet, as shown in Figures 3 and 4, have a comparatively small influence on the observed K_D, so in the calculation, a majoritic garnet composition is used (i.e., with 1 Al atom per formula unit), but the Fe-Mg partitioning is assumed to be the same as for pyrope-almandine garnet. Due to the simplifications made, the calculation is more likely to overestimate the narrowing of transformations due to the presence of garnet.

In Figure 6 the Fe content of olivine is observed to decrease slightly with pressure, which is consistent with an increase in the garnet-olivine K_D with pressure, as predicted by the model of O'Niell and Wood (1979). For a typical peridotitic bulk Fe/(Fe + Mg) ratio of 0.106, olivine on the low-pressure side of the olivine to wadsleyite transformation has an Fe/(Fe + Mg) ratio of approximately 0.09. Because the garnet-wadsleyite $K_D^{Fe\text{-}Mg}$ (=1.02) is lower than the garnet-olivine value (=1.78), wadsleyite on the high-pressure side of the transformation has an Fe/(Fe + Mg) ratio of approximately 0.105. This 1.5% shift in the Fe/(Fe + Mg) ratio of the $(Mg,Fe)_2SiO_4$ phase results in a narrowing of the transformation pressure interval by approximately 33% in comparison to the garnet free $(Mg_{0.9}Fe_{0.1})_2SiO_4$ transformation interval of 0.5 GPa (Fei and Bertka 1999). In the mantle, this shift would result in a seismic discontinuity 10 km wide as opposed to 15 km in a hypothetical garnet-free mantle. This calculated transformation interval is larger than the value of ~0.2 GPa (6 km) proposed in the previous experimental study of Irifune and Isshiki (1998). In this previous study, the Fe/(Fe + Mg) ratios of phases forming in a pyrolite peridotite composition were measured across the olivine to wadsleyite transformation. At these conditions, garnet and clinopyroxene were both present, however, as previously explained, because clinopyroxene is less Fe-rich than garnet, its presence cannot have a greater narrowing influence on the transformation than a similar quantity of garnet. When the same calculation is performed assuming that 30% garnet and 10% clinopyroxene are present, and using the clinopyroxene composition reported by Irifune and Isshiki (1998), the transformation is observed to be very slightly wider than when 40% garnet is assumed. The presence of clinopyroxene in the study of Irifune and Isshiki (1998) would not, therefore, have decreased the transformation interval any more than if only garnet were present. The discrepancies between the calculated Fe/(Fe + Mg) ratios shown in Figure 6 and those measured by Irifune and Isshiki (1998) are relatively small (~1%), however, even these differences have large effects on the determined width of the 410 km discontinuity, which is very sensitive to pressure and Fe/(Fe + Mg) ratio. It would seem difficult, therefore, to explain the ~66% narrowing of the transformation interval proposed for a peridotite composition by Irifune and Isshiki (1998) on the grounds of Fe-Mg partitioning into garnet and clinopyroxene.

The 410 km seismic discontinuity has been observed in studies on high-frequency reflected and converted waves (Benz and Vidale 1993), and is therefore predicted be at least locally very sharp, occurring over a depth interval of 4 km or less in some parts of the Earth. For the 410 km discontinuity to be caused by the olivine to wadsleyite transformation in a peridotite bulk composition, some additional influence other than the presence of a non-transforming phase must act, under certain conditions, to bring the experimentally determine width (10 km) into agreement with this seismic estimate. The mantle could, of course, have a lower olivine content, however, a 60:40 garnet:olivine mantle would still result in a transformation interval of 7 km. A non-linear yield during the transformation could make the seismically observed discontinuity appear sharper than the phase equilibria measurements (Helffrich and Wood 1996; Stixrude 1997). A further possibility, however, is that previous experimental determinations of Mg_2SiO_4-Fe_2SiO_4 transformations may have been influenced by the presence of even small levels of H_2O or Fe^{3+}. These components are frequently present in multianvil experiments, although they often go unrecognized, and are both likely to broaden experimental measurements of the olivine to wadsleyite transformation to a greater extent than probably occurs in the mantle. Although further work is required to explore fully these additional factors, it is quite likely that the olivine to wadsleyite transformation in the Earth's mantle can, under certain conditions, result in a sharp seismic discontinuity of 4 km or less.

Across the wadsleyite to ringwoodite transformation, the Fe content of the $(Mg,Fe)_2SiO_4$ phase shown in Figure 6 is calculated to increase from 0.10 on the wadsleyite side to approximately 0.11 on the ringwoodite side in a peridotite composition. This change of 1% in the Fe/(Fe + Mg) ratio results in a narrowing of the effective transformation interval by approximately 20% to 0.8 GPa from the garnet-free transformation of 1 GPa. In the mantle, this transformation would therefore take place over a depth interval of around 25 km. The 520 km discontinuity, which has been attributed to the wadsleyite-ringwoodite transformation, has been observed in low-frequency seismic studies (Revenaugh and Jordan 1991; Shearer 1996; Flanagan and Shearer 1998), but does not appear to reflect high-frequency seismic waves (Benz and Vidale 1993). This difference is consistent with a discontinuity greater than 10 km thick (Shearer 1996; Vidale 2001), which is then not inconsistent with the determined width of the wadsleyite to ringwoodite transformation made in this study.

ACKNOWLEDGMENTS

I thank G. Herrmannsdörfer, H. Fischer, H. Schultz, and D. Krauße for their technical assistance. I am also grateful to H. Huppertz who produced a peridotite glassed sample using his induction furnace. The manuscript benefited from the constructive reviews of H. O'Neill and an anonymous reviewer. H. O'Neill also kindly provided an invaluable preprint.

REFERENCES CITED

Akaogi, M. and Akimoto, S. (1977) Pyroxene-garnet solid-solution equilibria in the systems $Mg_4Si_4O_{12}$-$Mg_3Al_2Si_3O_{12}$ and $Fe_4Si_4O_{12}$-$Fe_3Al_2Si_3O_{12}$ at high pressure and temperatures. Physics of Earth and Planetary Interiors, 15, 90–106.

Akaogi, M., Ito, E., and Navrotsky, A. (1989) The olivine-modified spinel-spinel transitions in the system Mg_2SiO_4-Fe_2SiO_4: calorimetric measurements, thermochemical calculation, and geophysical application. Journal Geophysical Research, 94, 15671–15686.

Ballaran, T.B., Carpenter, M.A., Geiger, C.A., and Kozio, A.M. (1999) Local structural heterogeneity in garnet solid solutions. Physics and Chemistry of Minerals, 26, 554–569.

Benz, H.M. and Vidale, J.E. (1993) Sharpness of upper-mantle discontinuities determined from high-frequency reflections. Nature, 365, 147–150.

Fei, Y. and Bertka, C.M. (1999) Phase transformations in the Earth's mantle and mantle mineralogy. In Y. Fei, C.M. Bertka, and B.O. Mysen, Eds., Mantle Petrology: Field observations and High pressure experimentation: A Tribute to Francis R. (Joe) Boyd. The Geochemical Society, Special Publication no. 6, p. 189–207.

Flanagan, M.P. and Shearer, P.M. (1998) Global mapping of topography on the transition zone velocity discontinuities by stacking *SS* precursors. Journal of Geophysical Research, 103, 2673–2602.

Frost, D.J., Langenhorst, F., and van Aken, P.A. (2001) Fe-Mg partitioning between ringwoodite and magnesiowüstite and the effect of pressure, temperature and oxygen fugacity. Physics and Chemistry of Minerals 28, 455–470.

Geiger, C.A. and Feenstra A. (1997) Molar volumes of mixing of almandine-pyrope and almandine-spessartine garnets and the crystal chemistry and thermodynamic-mixing properties of the aluminosilicate garnets. American Mineralogist, 82, 571–581.

Hackler, R.T. and Wood, B.J. (1989) Experimental determination of Fe and Mg exchange between garnet and olivine and estimation of Fe-Mg mixing properties in garnet. American Mineralogist, 74, 994–999.

Harte, B., Harris, J.W., Hutchison, M.T., Watt G.R., and Wilding M.C. (1999) Lower mantle mineral associations in diamonds from São Luiz, Brazil. In Y. Fei, C. Bertka, and B.O. Mysen, Eds., Mantle Mineralogy: Field Observations and High Pressure Experimentation: A Tribute to Francis R. (Joe) Boyd. The Geochemical Society, Special Publication no. 6, p. 125–153.

Helffrich, G.R. and Wood, B.J. (1996) 410 km discontinuity sharpness and the form of the olivine phase diagram: resolution of apparent seismic contradictions. Geophysical Journal International, 126, 7–12.

Irifune, T. (1987) An experimental investigation of the pyroxene-garnet transformation in a pyrolite composition and its bearing on the constitution of the mantle. Physics of Earth and Planetary Interiors, 45, 324–336.

———(1994) Absence of an aluminous phase in the upper part of the lower mantle. Nature, 370, 131–133.

Irifune, T. and Isshiki, M. (1998) Iron partitioning in a pyrolite mantle and the nature of the 410-km seismic discontinuity. Nature, 349, 409–411.

Irifune, T. and Ringwood, A.E. (1993) Phase transformations in subducted oceanic crust and buoyancy relationships at depths of 600-800km in the mantle. Earth and Planetary Science Letters, 117, 101–110.

Katsura, T. and Ito, E. (1989) The system Mg_2SiO_4-Fe_2SiO_4 at high pressure and temperature: precise determination of stabilities of olivine, modified spinel and spinel. Journal of Geophysical Research, 94, 15663–15670.

O'Neill, H.St.C. and Wall, V.J. (1987) The olivine ortho-pyroxene spinel oxygen geobarometer, the nickel p recipitation curve, and the oxygen fugacity of the Earths upper mantle. Journal of Petrology, 8,1169–1191.

O'Neill, H.St.C. and Wood, B.J. (1979) An experimental study of Fe-Mg partitioning between garnet and olivine and its calibration as a geothermometer. Contributions to Mineralogy and Petrology, 70, 59–70.

O'Neill, H.St.C., Rubie, D.C., Canil, D., Geiger, C.A., Ross, C.R., Seifert, F., and Woodland, A.B. (1993) Ferric iron in the upper mantle and in transition zone assemblages: implications for relative oxygen fugacities in the mantle. Geophysical Monograph, 74 IUGG 14, 73–89.

O'Neill, H.St.C., Pownceby, M.I., and McCammon, C.A. (2003) The magnesiowüstite-iron equilibrium and its implications for the activity-composition relations of $(Mg,Fe)_2SiO_4$ olivine solid solutions. Contributions to Mineralogy and Petrology, in press.

Nishihara, Y. and Takahashi, E. (2001) Phase relations and physical properties of an Al-depleted komatiite to 23 GPa. Earth and Planetary Science Letters, 190, 65–77.

Revenaugh, J. and Jordan T.H. (1991) Mantle layering from S*c*S reverberations 2. The transition zone. Journal of Geophysical Research, 96, 19763–19780.

Ringwood, A.E. (1991) Phase transformations and their bearing on the constitution and dynamics of the mantle. Geochimica et Cosmochimica Acta, 55, 2083–2110.

Shearer, P.M. (1996) Transition zone velocity gradients and the 520-km discontinuity. Journal of Geophysical Research, 101, 3053–3066.

Stixrude, L. (1997) Structure and sharpness of phase transitions and mantle discontinuities. Journal of Geophysical Research, 102, 14835–14852.

Van Roermund, H.L.M., Drury, M.R., Barnhoorn A., and De Ronde A. (2001) Relict majoritic garnet microstructures from ultra-deep orogenic peridotites in western Norway. Journal of Petrology, 42, 117–130.

Von Seckendorff, V. and O'Neill, H.St.C. (1993) An Experimental study of Fe-Mg partitioning between olivine and ortho-pyroxene at 1173K, 1273K, and1423K and 1.6 GPa. Contributions to Mineralogy and Petrology, 113,196–207.

Vidale J.E. (2001) Peeling back the layers in Earth's mantle. Science, 294, 313.

Wiser, N.M. and Wood, B.J. (1991) Experimental determination of activities in Fe-Mg olivine at 1400K. Contributions to Mineralogy and Petrology, 108, 146–153.

Wood, B.J. (2000) Phase transformations and partitioning relations in peridotite under lower mantle conditions. Earth and Planetary Science Letters, 174, 341–354.

MANUSCRIPT RECEIVED MARCH 22, 2002
MANUSCRIPT ACCEPTED OCTOBER 22, 2002
MANUSCRIPT HANDLED BY THOMAS DUFFY